



# International Journal of Research in Academic World



Received: 09/January/2023

IJRAW: 2023; 2(2):140-144

Accepted: 03/February/2023

## Multiwavelength Study of Star Formation in NGC 3413

\*<sup>1</sup>SP Deshmukh and <sup>2</sup>AU Patil<sup>1</sup>Department of Physics, Institute of Science, Nagpur, Maharashtra, India.<sup>2</sup>Department of Physics, Rajaram College, Kolhapur, Maharashtra, India.

### Abstract

Early type galaxies (ETG), have regular impression of being “Red and Dead” with no ongoing star formation activity in it. But recent multiwavelength study of considerable fraction of ETGs suggests the active star formation in it. In the present work, we studied a lenticular galaxy NGC 3413. We performed optical spectroscopy and Spectral Energy Distribution study of target galaxy. It is found that, NGC 3413 holds an ongoing star formation activity and most of the stellar population of the galaxy is having age less than 2.5 Gyr. The star formation rate for target galaxy is found to be 0.64  $M_{\odot}$ /year. SED predicts the presence of moderate amount of dust in NGC 3413 with dust mass  $9.842 \times 10^5 M_{\odot}$ .

**Keywords:** Early type galaxies, star forming galaxies, SED fitting, Optical spectroscopy

### 1. Introduction

Early Early-type galaxies (ETGs) that include both ellipticals, as well as lenticular galaxies, have a regular impression of being featureless bulges that are devoid of dust and ISM with a lack of recent star formation activity. This class of galaxies occupies the red sequence on the Color-Magnitude plot. A general scenario is that in a CMD plane, a galaxy moves from the “blue-cloud” region, a region occupied by the star-forming, young, morphologically late-type galaxies to the non-star forming, passive red morphologically ETGs. The suppression of the star formation in ETGs is likely either due to the removal or heating of the cold gas supply essential for the star formation. However, this is not the whole and sole fate of the ETGs. The recent multiwavelength study suggests the presence of a considerable amount of star formation in so-called “Red & Dead” class of Early Type Galaxies (ETGs). It has been realized that a countable fraction of ETGs show the offset to this red sequence on the CMD plane and possess relatively bluer colors [1-3]. The blue ETGs not only differ in color from rest of the ETGs but several other factors confirm their distinction. The blue ETGs normally are seen more abundantly in the low-density environment with low-velocity dispersions [4]. Additionally, such systems were found to possess nonsymmetric color distribution [5] with a positive color gradient i.e. bluer centers unlike the common red ETGs [6].

In the present work, we carried out the multiwavelength study of star formation activity in NGC 3413. NGC 3413 is a nearby S0 edge-on galaxy with redshift 0.002151 and the T-parameter  $-1.1 \pm 2.4$ . This galaxy has been observed by GALEX, SDSS, CHANDRA, IRAS and many more missions, suggesting the presence of multiphase ISM in it. NGC 3413, as observed by SDSS, shows the presence of strong emission lines with a bluer continuum suggesting the presence of star formation activity in the target galaxy. Also, Sonbas et. al. (2018) studied NGC 3413 using X-ray Multi-Mirror Mission-Newton observation and observed that NGC 3413 holds a collection of many X-ray point-like sources with a diffuse X-ray emission. A bright ultraluminous X-ray source at its optical center is observed in the energy range of 0.3-10 KeV. Also, it is detected that a strong diffused  $H\alpha$  emission is present in the target galaxy. All these multiwavelength findings suggest the presence of strong star formation in this galaxy. IRAS detection of the target galaxy strongly suggests the presence of moderate amount of dust in it. The present study is carried out to study the star formation activity and the nature of the Spectral Energy Distribution of NGC 3413. The global parameters of galaxy NGC 3413 are listed in Table 1. This paper is organized as follows: Section 2 presents the data acquisition and analysis. Section 3 presents the main results and discussion. The main findings and the conclusion of the present work are discussed in Section 4. Throughout the work,

**Table 1:** Global parameters of NGC 3413

Alternate Names	UGC 05960; KUG 1048+330; 2MASS J10512070+3245598; GALEXASC J105120.75+324600.2; IRAS 10485+3301
RA; DEC	10h51m20.7s; 32h45m59s
Morphology	S0 edge-on
Mag B <sub>T</sub>	13.2
D <sub>25</sub>	1.71×0.86
Redshift	0.002151
Luminosity Distance	12.8 Mpc

we adopt a flat cosmological model with  $\Omega_M = 0.3$ ,  $\Omega_\Lambda = 0.7$  and  $H_0 = 70 \text{ km s}^{-1}$  and use the initial mass function of<sup>[7]</sup>.

## 2. Data Acquisition and Data Analysis

To cover the optical region of the electromagnetic spectrum for the target galaxy NGC 3413, we have made use of the imaging and spectroscopic data of Sloan Digital Sky Survey (SDSS). The optical imaging and spectroscopic data were obtained from the 7th data release of SDSS in u, g, r, i and z passbands with effective wavelengths of 3543Å, 4770Å, 6231Å, 7625Å, and 9134 Å<sup>[8, 9]</sup>. The angular resolution of the SDSS instrument is about 1.5 arcseconds. Here, we considered the Petrosian magnitudes<sup>[10]</sup>. Further to study the star formation process, we have made use of the Near-UV (175-275nm) and Far-UV (135-175nm) passband

data from Galaxy Evolution Explorer (GALEX) space mission. The GALEX data archive is controlled by the Multi-Mission Archive at the Space Telescope Science Institute (MAST). The angular resolution of GALEX imaging in FUV and NUV passbands is 4".2 and 5".3 respectively. The GALEX magnitudes are already calibrated to the AB magnitude system of<sup>[11]</sup> using the GALEX pipeline.

To cover the Infrared (IR) part of the spectral energy distribution of galaxies, we have made use of the data from the Two Micron All Sky Survey (2MASS) Extended Source Catalog (EXC)<sup>[12]</sup> for near-IR (J, H, Ks) passbands, the Wide-field Infrared Survey (WISE)<sup>[13]</sup> for mid-IR passbands and Infrared Astronomical Satellite (IRAS) faint source catalog data for the far-IR observations on the target galaxies. 2MASS covers the sky in three filters J, H and Ks with the central wavelengths of 1.232, 1.644, and 2.519  $\mu\text{m}$ , respectively. The WISE satellite has also observed the entire sky in four mid-IR bands: W1 (3.4  $\mu\text{m}$ ), W2 (4.6  $\mu\text{m}$ ), W3 (12  $\mu\text{m}$ ) and W4 (22  $\mu\text{m}$ ). WISE data provides valuable information regarding the stellar population, circumstellar dust and PAHs. To cover the far IR region of the electromagnetic spectrum, we used IRAS data. The Infrared Astronomical Satellite (IRAS) observatory enabled us to better constrain the peak of the SED in the IR and also to derive the temperature of the dust content of the sources. IRAS covers the infrared sky at 12, 25, 60 and 100  $\mu\text{m}$  wavelengths.

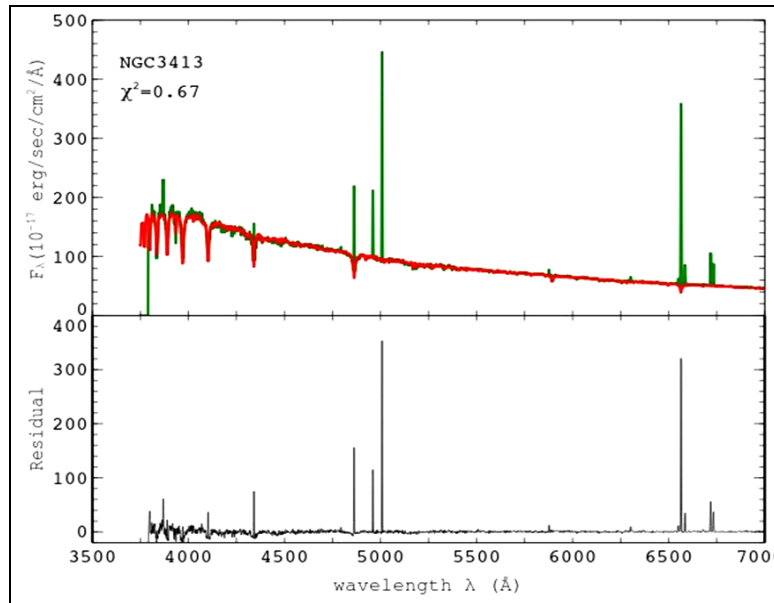


**Fig 1:** The rest frame optical spectrum of NGC 3413 fitted with the STARLIGHT code. The green line spectrum is observed spectrum. Red line spectrum is the model fitted by STARLIGHT. The bottom panel in figure indicates the residual spectrum.

### 2.1. Optical Spectroscopy and Stellar Population Synthesis

The optical spectrum of a galaxy is an excellent tool to determine the nature of the gas distribution and activity that may be present in the galaxy. Along with it, the optical spectrum is useful to determine the stellar population present in a galaxy. In the present study of the target galaxies, UGC 9519 and NGC 3699, the primary data reduction of SDSS spectrum is done with onedspec package in NOAO. The optical spectra of target galaxies were converted into the rest frame spectra using dopcor task. Spectra were also corrected for the Galactic extinction using deredden task. The stellar population synthesis is performed using STARLIGHT version 04 stellar population synthesis code<sup>[14, 15]</sup> and

REMOVEYOUNG spectral synthesis code of<sup>[16]</sup>. The linear combination of 45 SSP models was used from<sup>[17]</sup> libraries. This corresponds to a metallicity ( $Z$ ) of 0.2, 1, 2.5 in unit of solar metallicity that comprises fifteen types of stellar age combinations as 0.001, 0.00316, 0.005, 0.01, 0.025, 0.04, 0.102, 0.286, 0.640, 0.905, 1.434, 2.5, 5, 11 and 13 Gyr. The multiwavelength continuum flux which is free from the nebular emission contribution is used as an input to the REMOVEYOUNG code for further stellar population synthesis. This code takes care of removing the contribution from the stellar population younger than the adjustable cutoff age from the observed galaxy population. For this purpose, it uses the population vector information generated by the

STARLIGHT SPS model as an input. The population vector represents the mass fraction of the optimum stellar population mixture obtained by the SPS model, which depends on the age, metallicity and initial mass function (IMF) of the stellar population. We set  $t_{\text{cutoff}}$  to 0.1 Gyr. The deblending task is used to obtain the stellar absorption corrected fluxes of prominent emission lines in NGC 3413. The age wise distribution of stellar population in target galaxy NGC 3413 is as shown in figure 2.

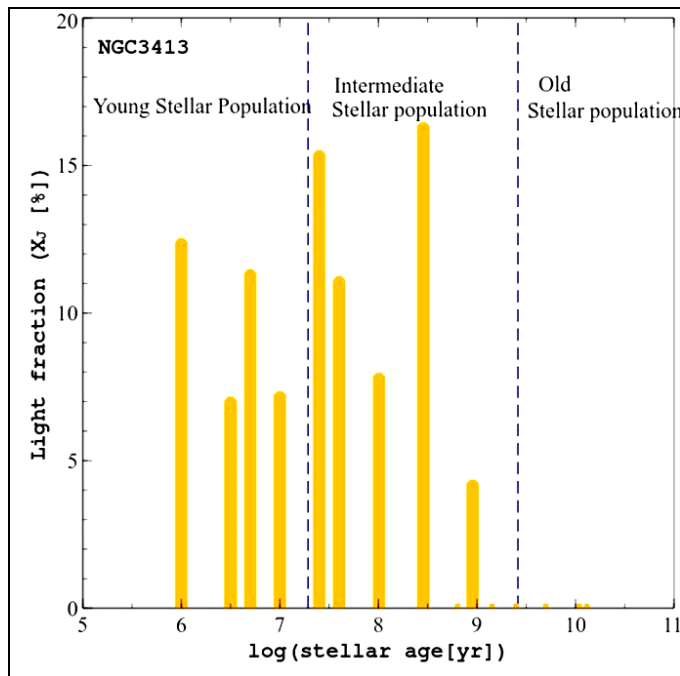


**Fig 2:** The age wise distribution of stellar population in target galaxy NGC 3413. Stars with age less than 25 Myr are treated as young stars whereas stars with age greater than 2.5 Gyr are treated as older stars.

## 2.2. SED Fitting

Fitting of the galaxy light over the full range of electromagnetic spectrum is essential to better constrain the properties of a galaxy. There are number of publicly available codes that are capable to fit the observed photometric data of a galaxy and provides a good estimate of various physical parameters of a galaxy. For the present galaxies, we used "Multi-wavelength Analysis of Galaxy Physical Properties" (MAGPHYS) [18] code to fit the observed SED of target galaxy. MAGPHYS is applicable for low as well as high redshift galaxies versions and are widely used by a large range of research community to study various physical properties of galaxies using broad band fluxes.

An empirical but physically motivated SED fitting code MAGPHYS makes use of the optical library of 50,000 models with varying star formation histories adopted from the 2007 version of [17] stellar population model and IR library of 50,000 models developed by [18] such that each IR model represents an optically thin modified black body emission from different grain sizes, temperature and emissivity indices. MAGPHYS take into account four types of dust components; the Polycyclic Aromatic Hydrocarbons (PAH) molecules, hot dust with a temperature range of 130-250 K, warm dust component in thermal equilibrium with a temperature range of 30-60K and cool dust with a temperature range of 15-25 K. Galactic-disk [7] initial mass function is employed while modeling the stellar emission SED. To rule out the effect of attenuation of star light by interstellar dust, a two-component

dust model developed by [19] is used. The resultant SED fit to the target galaxies is shown in Figure 3. The quality of the fit was checked from the  $\chi^2$  values. It is an indicator of the goodness of the model fit compared to the data points. The closer the  $\chi^2$  to 1, the better will be the fit. The physical parameters of a galaxy interpreted by MAGPHYS such as stellar mass, dust mass, star formation rate etc are given in Table 2.

**Table 2:** The star formation rate

Parameter	Description	Value
$f_{\mu}$	Fraction of total dust luminosity $L_{\text{dust}}$ contributed by the dust in ambient ISM $f_{\mu} = \frac{L_{\text{dust}}^{\text{ISM}}}{L_{\text{dust}}^{\text{Total}}}$	0.8475
$\tau_v$	Total optical depth seen by the young stars in stellar birth cloud	1.728
$\mu$	Fraction of the $\tau_v$ contributed by the dust in ISM $\mu = \frac{\tau_v^{\text{ISM}}}{(\tau_v^{\text{ISM}} + \tau_v^{\text{BC}})}$	0.45
$M_{\text{star}}$	Stellar mass in $M_{\odot}$	$1.48 \times 10^8 M_{\odot}$
$L_{\text{dust}}^{\text{Total}}$	Total Luminosity in $L_{\odot}$ absorbed by the dust	$2.11 \times 10^8 L_{\odot}$
$T_C^{\text{ISM}}$	Temperature of cold grains in thermal equilibrium in ISM in kelvin	17.9
$T_W^{\text{BC}}$	Temperature of warm grains in thermal equilibrium in birth clouds in kelvin	28.4
$M_d$	Dust mass in $M_{\odot}$	$9.842 \times 10^5$
$\Psi$	Star formation rate in $M_{\odot}/\text{year}$	0.16
$\psi_s$	Specific star formation rate in unit per year, $\psi_s = \Psi/M_{\text{star}}$	$1.54 \times 10^{-10}$

## 3. Results and Discussion

In the present study, we performed optical spectroscopy and SED fitting on early type galaxy NGC 3413. The main results of the study are as follows:

### i). Nature of central source in NGC 3413

The SDSS spectrum of target galaxy NGC 3413 shows the presence of prominent emission lines in the optical region of the galaxy. It suggests the presence of certain kind of activity. It may arise due to the presence of active galactic nucleus or due to the intense ongoing star formation. "Baldwin, Phillips & Terlevich" (BPT) diagrams [20] provides a tool to identify the nature of activity going on inside the galaxy. BPT diagram separates AGN from that of the star forming galaxies using the optical emission line ratios  $[\text{OIII}]\lambda 5007/\text{H}_{\beta} \lambda 4861$  and  $[\text{N II}]\lambda 6583/\text{H}_{\alpha} \lambda 6563$ .  $[\text{OIII}]\lambda 5007/\text{H}_{\beta} \lambda 4861$  is a good tracer of the degree of ionization and hence the temperature of emitting gas whereas, the line ratio  $[\text{N II}]\lambda 6583/\text{H}_{\alpha} \lambda 6563$  is sensitive to the lines originating from the ionized gas due to a high energy sources like the association of OB stars. As the emission lines used for deriving the BPT diagram are closely spaced, therefore, the corresponding integrated flux is independent of the internal galactic extinction and the aperture correction. Thus BPT diagram provides a reliable tool to classify Star forming galaxies from that of the AGNs. The position of NGC 3413 in BPT diagram is as shown in Figure 3. It clearly indicates the presence of intense star formation in the target galaxy. We used the [21] relation modified for the [7] IMF, to calculate the star formation rate as



$$\text{SFR} = \frac{L(H\alpha)}{2.1 \times 10^{41}} M_{\odot}/\text{yr}$$

Where,  $L(H\alpha)$  is the luminosity of  $H\alpha$  line in erg/s. It is corrected for internal dust extinction and the aperture correction. Using above relationship, the star formation rate in NGC 3413 is found to be **0.6435  $M_{\odot}/\text{year}$** .

### ii). Stellar Population Synthesis of NGC 3413

The stellar population Synthesis performed for the target galaxy NGC 3413 using STARLIGHT and REMOVEYOUNG code shows that most of the stellar population captured by the SDSS spectrum of NGC 3413 is of young to intermediate age. But the SDSS spectrum can cover only the central region of a galaxy. For NGC 3413, SDSS spectrum capture only 13% of the total galaxy light. Thus, as predicted by stellar population synthesis, the stellar population in the central region of NGC 3413 is of young to intermediate age. This result supports the star forming nature of central source in the target galaxy as discussed in section 3.1.

### iii). SED Fitting Results

The spectral energy distribution study of target galaxy NGC 3413 using the UV-optical-IR data and the MAGPHYS code is as shown in figure 4. It interpreted various physical parameters of the target galaxy as shown in table 2. The star formation rate predicted by SED fitting is in good agreement to that of the  $H\alpha$  emission line based star formation rates. The dust mass in NGC 3413 is predicted to be  $9.842 \times 10^5 M_{\odot}$ , thus indicating the presence of moderate amount of dust in this dwarf elliptical galaxy. A careful look into the SDSS images of NGC 3413 shows the presence of patchy dust in NGC 3413. One need the optical observations of NGC 3413 with a powerful high resolution telescopes to predict the special distribution of dust in the target galaxy. In many galaxies, dust and the star forming regions are found to be specially coaligned, suggesting the common origin of both of the components.

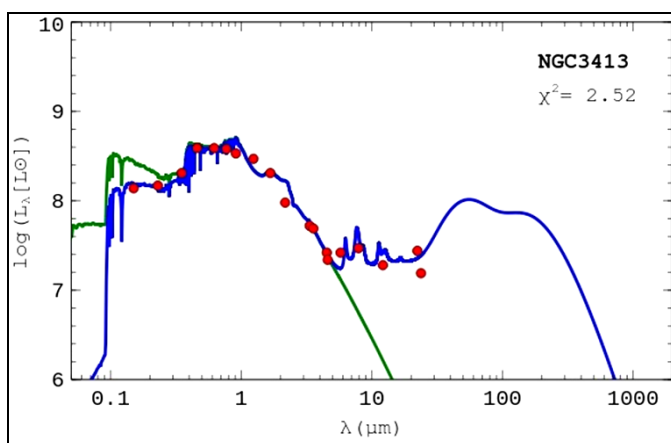


**Fig 3:** SED fitting on photometric data of the target galaxy NGC 3413. Attenuated and unattenuated spectra are shown in green and blue color respectively. Red points show photometric data points used for SED fitting.

### 4. Conclusion

In the present work, we performed the optical spectroscopy and SED fitting of target galaxy with the aim to study the nature of activity taking place inside it. The BPT diagram clearly suggest the star formation activity present on the target galaxy. The stellar population synthesis performed using the

STARLIGHT and REMOVEYOUNG code also supports the presence of young stellar population in NGC 3413. The SFR predicted by SED fitting is found to be  $0.16 M_{\odot}/\text{year}$  which is in good agreement with the SFR calculated using  $H\alpha$  emission line flux. SED fitting also suggests the presence of moderate amount of dust in NGC 3413. The dust mass is found to be  $9.842 \times 10^5 M_{\odot}$ .

### 5. Acknowledgement

The present work used the data from various sites such as NASA extragalactic database, SDSS, GALEX, 2MASS, IRAS, WISE. SPD is very much thankful to all institutes/organizations maintaining these databases. This work used various analysis facilities such as IRAF, MAGPHYS, STARLIGHT, REMOVEYOUNG. SPD is very much thankful to the founders of these codes.

### References

1. Kannappan SJ, Guie JM, Baker AJ. E/S0 Galaxies on the Blue Color-Stellar Mass Sequence at  $z = 0$ : Fading Mergers or Future Spirals? *\aj*. 2009; 138:579-597.
2. Yi SK, Yoon SJ, Kaviraj S, Deharveng JM, Rich RM, Salim S *et al*. Galaxy Evolution Explorer Ultraviolet Color-Magnitude Relations and Evidence of Recent Star Formation in Early-Type Galaxies. *\apj*. 2005; 619:L111-L114.
3. Faber SM, Willmer CNA, Wolf C, Koo DC, Weiner BJ, Newman JA, Im M, Coil AL, Conroy C, Cooper MC, *et al*. Galaxy Luminosity Functions to  $z \sim 1$  from DEEP2 and COMBO-17: Implications for Red Galaxy Formation. *\apj*. 2007; 665:265-294.
4. Schawinski K, Lintott C, Thomas D, Sarzi M, Andreescu D, Bamford SP, Kaviraj S, Khochfar S, Land K, Murray P *et al*. Galaxy Zoo: a sample of blue early-type galaxies at low redshift\*. *\mnras*. 2009; 396:818-829.
5. Lee JH, Lee MG, Hwang HS. The Nature of Blue Early-Type Galaxies in the GOODS Fields. *\apj*. 2006; 650:148-165.
6. Ge C, Gu QS. Peculiar early-type galaxies with central star formation. *Res. Astron. Astrophys*. 2012; 12:485-499.
7. Chabrier G. Galactic Stellar and Substellar Initial Mass Function. *\pasp*. 2003; 115:763-795.
8. Fukugita M, Ichikawa T, Gunn JE, Doi M, Shimasaku K, Schneider DP. The Sloan Digital Sky Survey Photometric System. *\aj*. 1996; 111:1748.
9. Gunn JE, Sigmund WA, Mannery EJ, Owen RE, Hull CL *et al*. The 2.5 m Telescope of the Sloan Digital Sky Survey. *\aj*. 2006; 131:2332-2359.
10. Abazajian KN, Adelman-McCarthy JK, Agüeros MA, Allam SS, Allende Prieto C, An D, Anderson KSJ, Anderson SF, Annis J, Bahcall NA, *et al*. The Seventh Data Release of the Sloan Digital Sky Survey. *\apjs*. 2009; 182:543-558.
11. Oke JB, Gunn JE. Secondary standard stars for absolute spectrophotometry. *\apj*. 1983; 266:713-717.
12. Skrutskie MF, Cutri RM, Stiening R, Weinberg MD, Schneider S, Carpenter JM *et al*. The Two Micron All Sky Survey (2MASS). *\aj*. 2006; 131:1163-1183.
13. Wright EL, Eisenhardt PRM, Mainzer AK, Ressler ME, Cutri RM, Jarrett T, Kirkpatrick JD *et al*. The Wide-field Infrared Survey Explorer (WISE): Mission Description and Initial On-orbit Performance. *\aj*. 2010; 140:1868-1881.

14. Cid Fernandes R, Mateus A, Sodr  L, Stasińska G, Gomes JM. Semi-empirical analysis of Sloan Digital Sky Survey galaxies-I. Spectral synthesis method. *\mnras*. 2005; 358:363-378.
15. Mateus A, Sodr  L, Cid Fernandes R, Stasińska G. Semi-empirical analysis of Sloan Digital Sky Survey galaxies-IV. A nature via nurture scenario for galaxy evolution. *\mnras*. 2007; 374:1457-1472.
16. Gomes JM, and Papaderos P. RemoveYoung: A tool for the removal of the young stellar component in galaxies within an adjustable age cutoff. *\aap*. 2016; 594:A49.
17. Bruzual G, Charlot S. Stellar population synthesis at the resolution of 2003. *\mnras*. 2003; 344:1000-1028.
18. Da Cunha E, Charlot S, Elbaz D. A simple model to interpret the ultraviolet, optical and infrared emission from galaxies. *\mnras*. 2008; 388:1595-1617.
19. Charlot S, Fall SM. A Simple Model for the Absorption of Starlight by Dust in Galaxies. *\apj*. 2000; 539:718-731.
20. Baldwin JA, Phillips MM, Terlevich R. Classification parameters for the emission-line spectra of extragalactic objects. *\pasp*. 1981; 93:5-19.
21. Kennicutt Jr, RC. Star Formation in Galaxies along the Hubble Sequence. *\araa*. 1998; 36:189-232